

# Differentiating Round Pneumonia from Malignant Lung Masses Using Histogram-Based Image Analysis

Hasan Genç<sup>1\*</sup>, Murat Baykara<sup>2</sup>

<sup>1</sup>Elazığ Fethi Sekin City Hospital

<sup>2</sup>İstanbul Haydarpaşa Numune Training and Research Hospital

## ABSTRACT

Round pneumonia is characterized by round, well-circumscribed infiltrative lesions on computed tomography (CT) that can mimic malignant lung masses. This study aimed to evaluate distinguishing parameters between round pneumonia and primary malignant lung masses using histogram-based image analysis, and to investigate the diagnostic contribution of this method.

In this retrospective study, 60 patients (30 with round pneumonia, 30 with primary malignant lung mass) diagnosed between 2020 and 2024 were included. Unenhanced thoracic CT images were analyzed; lesions were assessed by two radiologists, and a circular region of interest (ROI) was selected on an appropriate slice for each lesion. Histogram and texture analysis parameters obtained from these ROIs were compared between the two groups. The Mann-Whitney U test was used for two-group comparisons and Spearman's rank test for correlation ( $p < 0.05$ ).

Histogram-based analysis revealed many parameters with statistically significant differences between round pneumonia and malignant lung masses. In particular, features such as standard deviation, variance, entropy, range, interquartile range, and contrast provided significant separation between the two groups ( $p < 0.001$ ). On receiver operating characteristic (ROC) analysis, histogram variance achieved the highest diagnostic performance, distinguishing pneumonia vs. tumor with 100% sensitivity and 100% specificity (AUC = 1.00, threshold  $\approx 1.91 \times 10^3$  HU<sup>2</sup>). No significant correlation was found between the standardized uptake value (SUV) and any histogram parameter in the tumor group.

CT histogram analysis is a useful non-invasive tool for distinguishing round pneumonia from malignant lung lesions with similar imaging features, potentially reducing unnecessary invasive procedures.

**Keywords:** CT histogram analysis; Lung cancer; Round pneumonia

## Introduction

Round pneumonia is a form of lobar pneumonia observed as a round-shaped consolidation on imaging, often resulting from the containment of infection spread via Kohn's pores and Lambert's canals (1). Its imaging findings usually appear as well-defined, homogeneously dense solid consolidations, and thus it can be confused with malignant lung masses on radiologic exams (2). In adults, these types of round lesions can suggest malignancy and lead to diagnostic confusion. Therefore, there is a need to develop non-invasive, objective methods to distinguish between these two entities.

Among malignant lung lesions, the most common type is non-small cell lung cancer (NSCLC). Lung cancer is one of the leading causes of cancer-related deaths worldwide (3). It is the most common cancer in men and the second most common in women, with a five-year survival rate of only around 16% (4). Numerous factors,

especially tobacco use, as well as environmental and occupational exposures, play a role in its etiology (3,4).

Among imaging techniques, computed tomography (CT) is the primary diagnostic tool for evaluating lung lesions. CT, with its high spatial resolution, can assess solid, part-solid, or cystic lesions in detail and provides information on both morphological characteristics and density parameters (5). However, in some cases the CT appearances of benign and malignant lesions can overlap, leading to diagnostic uncertainty.

Histogram-based image analysis is a method that statistically evaluates the pixel-by-pixel distribution of attenuation values obtained from CT images. By using many parameters such as mean, median, variance, entropy, skewness, and kurtosis, one can infer tissue homogeneity, heterogeneity, and structural characteristics (6,7). In recent years, studies have shown that such analysis methods provide significant contributions in characterizing tissue differences and in

\*Corresponding Author: Hasan Genç, Elazığ Fethi Sekin City Hospital, Radiology Department  
Email: dr.hsgnc@gmail.com, Phone: 0 (553) 610 05 95

ORCID ID: Hasan Genç: 0009-0002-6366-3146, Murat Baykara: 0000-0003-2588-9013

Received: 17.06.2025, Accepted: 02.03.2026

distinguishing malignant from benign lesions (8,9). Notably, integrating histogram data with texture analysis has been reported to increase diagnostic accuracy in lesions that are difficult to differentiate on imaging alone (10). In this context, the aim of our study was to investigate whether round pneumonia and primary malignant lung masses can be differentiated using histogram parameters derived from CT images.

## Materials and Methods

This retrospective study protocol was approved by the Institutional Ethics Committee. Patients diagnosed with round pneumonia ( $n = 30$ ) or NSCLC lung cancer ( $n = 30$ ) between 2020 and 2025 were identified from the hospital database. The inclusion criteria were as follows: a confirmed diagnosis of round pneumonia or a primary lung mass at our institution during the specified period, availability of at least one high-quality thoracic CT scan stored in the hospital archive, complete clinical and radiological data in the records, and age of 18 years or older. The exclusion criteria were: absence of a definitive histopathological diagnosis for the lung mass, low-quality or artifact-laden CT images, incomplete clinical or treatment documentation, patients under the age of 18, any history of extrathoracic malignancy not clearly related to the pulmonary lesion, the presence of non-infectious etiologies for the lesion such as granulomatous disease, vasculitis, or metastasis, and cases with multiple pulmonary lesions in which individual evaluation was not possible. In the round pneumonia group, all patients showed clinical and radiological improvement following antibiotic therapy, and regression of the lesion was confirmed by follow-up imaging. In the lung cancer group, only patients with histopathologically confirmed NSCLC were included, consisting of adenocarcinoma ( $n = 14$ ), large cell carcinoma ( $n = 7$ ), and sarcomatoid carcinoma ( $n = 5$ ), pleural mesothelioma ( $n = 4$ ) subtypes (Figure 1).

71 patients with mass-like lesions on thoracic CT, 11 were excluded due to lack of histopathological diagnosis ( $n=4$ ), poor-quality or artifact-containing/incomplete CT images ( $n=3$ ), and insufficient clinical or treatment-related data ( $n=4$ ). The final study population included 60 patients, comprising 30 with non-small cell lung cancer (adenocarcinoma, large cell carcinoma, sarcomatoid carcinoma, and pleural mesothelioma) and 30 with round pneumonia.

All thoracic CT examinations were performed using a 128-slice CT scanner (Ingenuity Core 128; Philips Medical Systems, Best, Netherlands). Axial images were acquired from the thoracic inlet to the mid-kidney level in a craniocaudal direction. Scans were obtained without intravenous contrast using the following parameters: 100 kVp; 100–170 mA (with automatic tube current modulation);  $2 \times 2$  mm collimation; 0.5 mm slice thickness; and 1 mm isotropic voxel size. The images were evaluated by two radiologists (H.G. and M.B.). Image data were exported from the hospital PACS (Picture Archiving and Communication System) in DICOM format and transferred to a Windows-based computer in XML format, then loaded into a custom algorithm developed in MATLAB (via Microsoft Excel). For histogram analysis, a circular ROI was selected on the slice where the lesion was most prominent for each patient (Figures 2 and 3).

Based on lesion dimensions observed on axial CT slices, the mean lesion diameter was  $36 \pm 16.3$  mm in the tumor group and  $34.5 \pm 9.4$  mm in the pneumonia group; this difference was not statistically significant ( $p = 0.71$ ). The ROI size was optimized considering these lesion dimensions so as not to disrupt the intralesional morphological integrity while adequately capturing tissue heterogeneity, and was applied uniformly for all patients. Accordingly, a circular ROI with a diameter of 10 mm was used for all lesions.

Various histogram and texture parameters were derived from each lesion's ROI. These included first-order (histogram-based) metrics—such as mean, median, variance, standard deviation, entropy, skewness, and kurtosis—and second-order texture features such as contrast (from the gray-level co-occurrence matrix, GLCM), energy, homogeneity, and high gray-level run emphasis (from the gray-level run length matrix, GLRLM), among others.

**Statistical Analysis:** Although this was a retrospective study, a reference sample size estimation was performed using G\*Power software (version 3.1.9.7) to ensure adequate statistical power. Assuming a large effect size (Cohen's  $d = 0.8$ ),  $\alpha = 0.05$ , and a desired power of 0.70, the estimated minimum sample size was

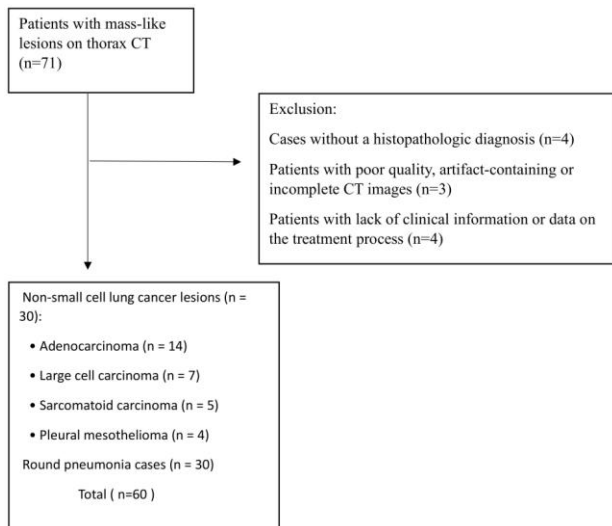


**Fig. 1.** Flowchart of patient selection

26 subjects per group. With 30 patients included in each group, the final cohort met this threshold, thereby supporting the statistical validity of the comparisons. All statistical analyses were performed using SPSS Statistics 22 (IBM Corp., Chicago, IL). Descriptive data for categorical variables were presented as counts (n) and percentages (%), and for continuous variables as median values with interquartile range (IQR). Group comparisons for categorical variables were made with the Pearson chi-square test. The distribution of continuous variables was assessed with the Kolmogorov-Smirnov test. The Mann-Whitney U test was used to compare continuous variables between the two groups. Spearman's rank correlation test was used to examine relationships between quantitative variables. A p value < 0.05 was considered statistically significant.

In addition, a receiver operating characteristic (ROC) analysis was performed to determine the histogram parameter with the highest discriminative capability. The area under the ROC curve (AUC) was calculated for each parameter, and the optimal threshold was determined for the most discriminative parameter. Using this threshold, the corresponding sensitivity and specificity were reported.

## Results

A total of 60 patients were included, with 30 patients in the round pneumonia group and 30 in

the NSCLC tumor group. In terms of gender distribution, the tumor group had 5 females (16.7%) and 25 males (83.3%), while the pneumonia group had 10 females (33.3%) and 20 males (66.7%); this difference was not statistically significant ( $p = 0.097$ ). The mean age was  $65.2 \pm 12.3$  years in the tumor group and  $37.7 \pm 13.6$  years in the pneumonia group, and this difference was statistically significant (Table 1). Based on axial CT imaging, the average lesion diameter was  $36 \pm 16.3$  mm in the tumor group and  $34.5 \pm 9.4$  mm in the pneumonia group, which was not a significant difference ( $p = 0.71$ ).

CT histogram and texture analysis revealed several parameters with statistically significant differences between the round pneumonia and malignant tumor groups. The primary parameters that showed significant differences included standard deviation, median, mean absolute deviation, median absolute deviation, variance, range, interquartile range (IQR), and entropy among the histogram-based metrics, as well as contrast (GLCM), run length nonuniformity (GLRLM), and high gray-level run emphasis (GLRLM) among the texture analysis features. By contrast, certain histogram parameters such as skewness, most frequent value, uniformity, and correlation were not statistically significant between the two groups ( $p > 0.05$ ) (Table 2).

To evaluate the discriminatory ability of each parameter, ROC analysis was performed for differentiating the pneumonia and tumor groups (each group  $n = 30$ ). For each parameter, ROC curves were generated and the AUC, optimal threshold, and corresponding sensitivity and specificity were calculated. Histogram variance emerged as the most powerful single discriminator, with an AUC of 1.00. Using a threshold of approximately 1912.68 ( $\approx 1.91 \times 10^3$  HU<sup>2</sup>), histogram variance achieved 100% sensitivity and 100% specificity, indicating perfect separation of the pneumonia and tumor cases. The run length nonuniformity (RLN) feature had an AUC of about 0.79, indicating moderate-to-high discriminative power, and high gray-level run emphasis (HGRE) had an AUC of around 0.65, indicating lower discriminative performance (Figure 4). On the other hand, parameters such as histogram entropy, IQR, and mean absolute deviation yielded AUC values below 0.60,

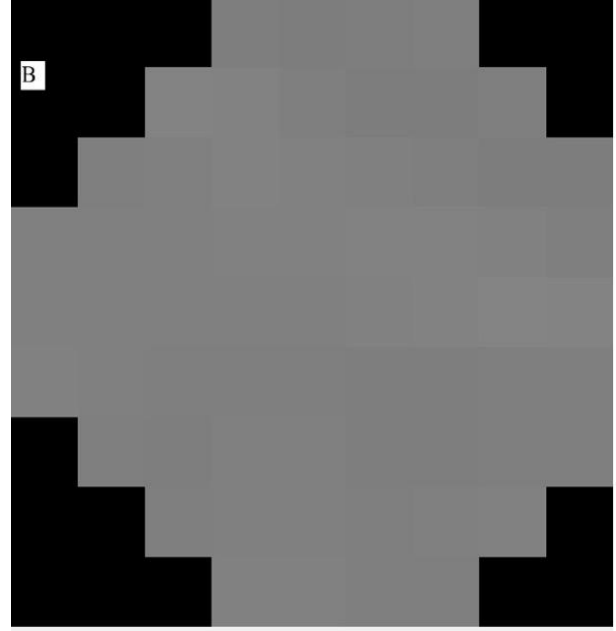
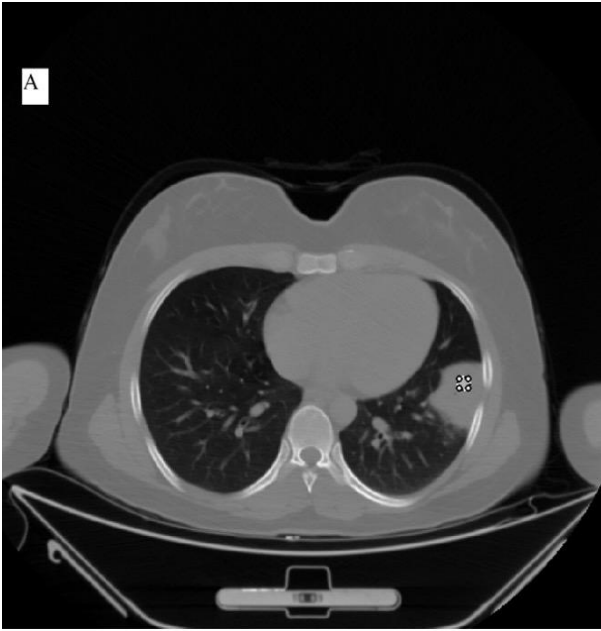


**Fig. 2.** A,B. ROI Selection and Retrieval from the lesion area from axial DICOM [Digital Imaging and Communications in Medicine] Image of a patient with round pneumonia

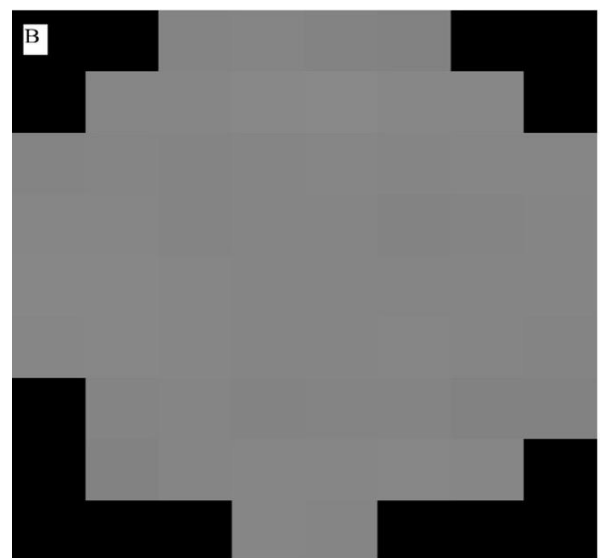
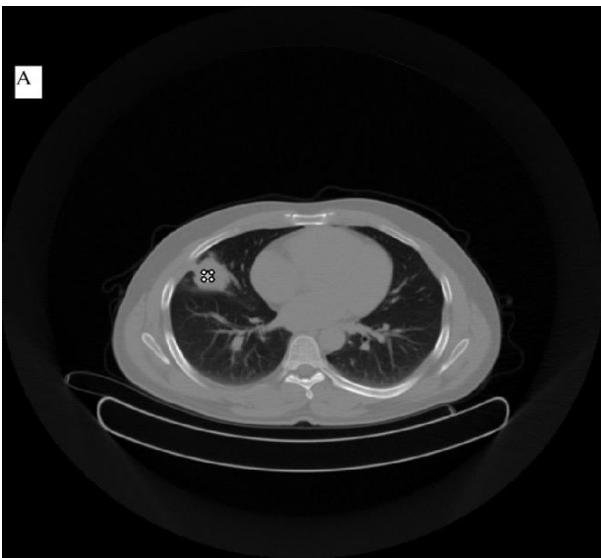


**Fig. 3.** A,B. ROI Selection and Retrieval from the lesion area from axial DICOM [Digital Imaging and Communications in Medicine] Image from a patient diagnosed with a mass in the lung

reflecting poor (near-random) discriminative ability. These results suggest that those particular parameters provide little to no clinical value in distinguishing round pneumonia from a malignant lesion. Some other parameters (for example, histogram standard deviation, median absolute deviation, and GLCM contrast) showed intermediate discrimination with AUCs on the order of  $\sim 0.75$ ; for these, the sensitivity and specificity were generally in the range of 70–80%. Overall, histogram variance stood out as by far the strongest differentiating feature. While RLN and HGRE were not individually very strong

predictors, they may offer incremental value when multiple features are combined in a model. However, if a single parameter is to be used in clinical practice, histogram variance would be the most reliable choice given its superior diagnostic performance.

Figure 4. Comparison of ROC curves for three different parameters. Histogram variance (orange curve) demonstrates excellent discrimination with  $AUC = 1.00$ , whereas RLN (yellow-orange curve) shows moderate-to-high discrimination ( $AUC \approx 0.79$ ) and HGRE (red curve) shows low-to-

**Table 1:** Comparison of Demographic Characteristics of The Groups

		Mass [n=30]		Pnömonia [n=30]		P
		Sayı	%	Sayı	%	
Gender	Female	5	16,7	10	33,3	0,097*
	male	25	83,3	20	66,7	
Age, Median [IQR]		65,23±12,30		37,70±13,55		<0,001**

IQR=Interquartile Range\*Chisquare analysis, \*\*Mann Whitney U test was applied

**Table 2:** Comparison of Histogram-Based Parameters Between The Pneumonia and Tumor Groups

	Mass [n=30]		Pnömonia [n=30]		p*
	Median [IQR]		Median [IQR]		
Standard Deviation of Histogram	12,21 [10,05-15,93]		52,54 [46,73-57,58]		<0,001
Mean Absolute Deviation of Histogram	9,45 [7,91-12,86]		41,46 [37,69-46,64]		<0,001
Median Absolute Deviation of Histogram	7,00 [6,00-10,50]		35,50 [34,00-40,50]		<0,001
Variance of Histogram	149,20 [100,98-253,82]		2761,36 [2183,53-3315,28]		<0,001
Range of Histogram	66,50 [56,00-76,00]		302,00 [235,00-339,00]		<0,001
Interquartile Range of Histogram	15,00 [12,00-21,00]		72,00 [65,50-80,50]		<0,001
Most Frequent Value of Histogram	1054,00 [1046,00-1064,00]		1052,00 [1030,00-1063,00]		0,416
Skewness of Histogram	-0,06 [-0,32-0,17]		-0,01 [-0,16-0,07]		0,745
Entropy of Histogram	5,17 [4,89-5,60]		6,75 [6,28-6,87]		<0,001
Uniformity of Histogram	0,30 [0,27-0,37]		0,29 [0,27-0,33]		0,315
Contrast of Matrix	24,75 [15,67-37,18]		38,67 [26,26-78,00]		0,006
Correlation of Matrix	0,00 [-0,01-0,02]		0,00 [-0,20-0,01]		0,249
Run Length Nonuniformity of GLRLM 000°	16,27 [12,52-19,82]		20,45 [13,52-27,95]		0,021
High Gray-Level Run Emphasis of GLRLM 000°	61,07 [43,35-83,27]		84,58 [55,00-180,24]		0,008

\*Abbreviations: GLRLM= Gray Level Run Length Matrix; IQR= Interquartile Range

Note: Statistically significant values are indicated in bold and italics

moderate discrimination (AUC  $\approx$  0.65). Notably, histogram variance provides the highest classification accuracy compared to the other two parameters.

Furthermore, no significant correlation was found between the standardized uptake value (SUV) and any of the histogram parameters in the tumor group.

## Discussion

Lung masses are generally malignant lesions, whereas round pneumonia is a benign inflammatory condition. These two clinical entities can display similar radiologic appearances, and thus their differentiation is not always straightforward. This is especially true for round or oval lesions observed in adults, which can be mistaken for malignancies on imaging (11). To

establish a differential diagnosis, patients are often subjected to invasive procedures such as biopsy or to imaging modalities involving ionizing radiation like PET/CT (positron emission tomography/computed tomography).

However, on PET/CT imaging both malignant lesions and certain inflammatory processes (for example, organizing pneumonia) can show FDG (fluorodeoxyglucose) uptake, which limits the ability of PET/CT to distinguish between them (12). Therefore, quantitative imaging methods such as histogram analysis are needed to achieve a more reliable differentiation between benign and malignant lesions that have similar radiologic presentations. Histogram-based texture analysis, by evaluating the distribution of pixel intensities within a lesion, can contribute to differentiating between different pathologies (13). However, since our analysis was performed on a single representative axial slice using a fixed-size ROI,

this approach may not fully represent the three-dimensional intralesional heterogeneity of the lesion. In our study, several histogram-based parameters—such as standard deviation, mean absolute deviation, median absolute deviation, variance, range, interquartile range, and entropy—emerged as strong indicators reflecting the greater tissue heterogeneity of malignant lesions. These parameters respectively represent the spread of the intensity distribution, the magnitude of deviations from the mean, the variability centered around the median, the overall intensity variance, the difference between minimum and maximum intensities, the spread of the middle 50% of intensities, and the degree of structural disorder; each showed a highly significant difference ( $p < 0.001$ ) between malignant and benign lesions. Additionally, texture-derived parameters including contrast (from GLCM), run length nonuniformity (RLN), and high gray-level run emphasis (HGRE) (the latter two from GLRLM) were significantly different between the groups, reflecting differences in intralesional microstructural organization, intensity contrast, and the continuity of high-intensity structures in malignant tissue (see Table 2). Each of these parameters is a statistical descriptor highlighting a different aspect of tissue heterogeneity. In order to better understand their significance and role in evaluating malignant lesions, each key parameter is briefly explained below:

Standard deviation (SD) measures the dispersion of pixel intensity values within a lesion. Malignant lesions typically exhibit heterogeneous structures, resulting in a broader distribution of CT attenuation values, and SD has been reported as statistically significant in distinguishing lung tumors from benign lesions (13). Mean absolute deviation quantifies the average deviation of intensities from the mean and better reflects the heterogeneity present in malignant lesions, which often contain more spatial variation; this metric has been associated with malignancy in the literature (14). Median absolute deviation (MedAD), a variation measure more resistant to outliers, is valuable in identifying malignant lesions that frequently include extreme voxel values (15). Variance, which represents the overall spread of intensity values, is typically elevated in malignant lesions due to their microstructural complexity, and in our study, it emerged as the most discriminative histogram parameter for distinguishing round pneumonia from malignant lesions (16). Range, reflecting the difference between minimum and maximum intensity values,

tends to be wider in malignant masses, indicating greater structural diversity (17). The interquartile range (IQR), which evaluates the dispersion of the middle 50% of intensities, has been shown to be useful in differentiating round pneumonia from malignant lung masses (18). Entropy captures the randomness or textural complexity of a lesion's intensity distribution; higher entropy values are indicative of the irregular and heterogeneous composition characteristic of malignancies, and its role in lung cancer diagnosis and prognosis has been emphasized (19). Contrast, a feature derived from the gray-level co-occurrence matrix (GLCM), quantifies local intensity differences between neighboring pixels and is often higher in malignant tissues, reflecting sharper transitions and microvascular alterations (20). Run length nonuniformity (RLN), based on the gray-level run length matrix (GLRLM), assesses variability in the length of contiguous pixel runs with similar intensities, and it is significantly increased in malignant lesions due to nonuniform internal architecture (21). Lastly, high gray-level run emphasis (HGRE), also derived from GLRLM, evaluates the continuity of high-intensity voxel clusters and is typically elevated in malignant tissues with hyperdense components, further supporting its utility in identifying aggressive tumors (22). Furthermore, Zhang et al. (23) examined various statistical parameters using histogram analysis to differentiate round pneumonia from lung adenocarcinoma, demonstrating the utility of such quantitative features for distinguishing these conditions.

Among all the parameters we evaluated, histogram variance was found to have the highest diagnostic accuracy. Although our study was retrospective in design, the adequacy of the sample size was evaluated with reference to a power analysis assuming a large effect size. Including 30 patients in each group meets the minimum estimated sample size requirement and supports the statistical reliability of the findings despite the limited cohort size. Histogram variance is a fundamental radiomic feature that reflects the degree of intensity heterogeneity within a lesion. In our study, histogram variance achieved an AUC of 1.00 with 100% sensitivity and specificity in differentiating round pneumonia from a malignant lung mass. This finding indicates that variance very effectively captures intralesional tissue differences and can distinguish inflammatory infiltrates from neoplastic tissue. It is worth noting that while histogram variance demonstrated perfect discriminative ability (AUC = 1.00), this

result must be interpreted with caution. The relatively small and balanced sample size ( $n = 30$  per group) may predispose the model to **overfitting**, meaning it may perform exceptionally well on the current dataset but fail to generalize to external or more heterogeneous populations. Such ideal classification outcomes are uncommon in larger, real-world clinical settings, suggesting that validation with independent and multicenter cohorts is essential to verify the robustness and reproducibility of this finding. Consistent with our results, Zhang et al. (24) reported that histogram variance possesses high discriminative power for differentiating malignant pulmonary nodules. Additionally, Rao et al. (25) emphasized that histogram-based parameters—especially variance—make important contributions in identifying microstructural differences across various lung pathologies. In light of these observations, histogram variance stands out as a key variable that should be prioritized in computer-aided diagnostic systems as well as in clinical radiological evaluation.

Overall, our findings demonstrate that histogram-based analysis can provide significant quantitative differentiation between benign and malignant lung lesions. The ability of histogram features to distinguish benign round pneumonia from malignant lung masses enables more accurate diagnoses and helps avoid unnecessary invasive procedures (such as biopsies) for patients. In particular, the application of advanced imaging techniques like CT texture analysis has notably improved the diagnostic accuracy for serious conditions like lung cancer. Prior studies have similarly noted that histogram-derived parameters, by capturing tumor microvascular architecture and tissue heterogeneity, effectively prevent benign infection-related lesions (like round pneumonia) from being misinterpreted as malignancies (13). Despite these promising findings, the statistically significant age difference between the pneumonia and malignancy groups represents a potential confounding factor that may have influenced CT histogram parameters. Age-related changes in lung parenchyma can affect tissue heterogeneity and attenuation distribution. Future studies employing age-matched cohorts or age-adjusted analyses may help to better clarify the independent effect of histogram-based parameters.

Another important clinical benefit of histogram-based analysis is its potential to facilitate early diagnosis. For diseases such as lung cancer, diagnosing at an early stage significantly increases the chances of successful treatment. The ability of

histogram parameters to distinguish benign from malignant lesions can accelerate the diagnostic process and, through earlier intervention, improve patient outcomes. In our study, histogram parameters showed significant differences in malignant lesions; this parallels findings in the literature that the histological and microvascular heterogeneity of malignancies can be accurately captured by parameters like standard deviation, variance, and entropy (26). Early diagnosis is especially critical for small lesions and can greatly impact patients' quality of life and long-term survival.

Non-invasive diagnostic methods are a cornerstone of radiologic practice, as they reduce the number of invasive procedures and protect patients from unnecessary risks. CT histogram analysis offers a non-invasive, quantitative approach, which can make clinical practice safer and more patient-friendly. Considering that invasive procedures such as biopsy or even PET/CT scans can lead to serious complications in some patients, the necessity and benefit of histogram-based imaging analyses become even more apparent. In our study, the fact that benign and malignant conditions could be differentiated by histogram parameters suggests that this method provides a potentially safer and effective alternative for patient evaluation.

Histogram-based analyses have also been reported to play an important role in prognostication. Parameters such as entropy, skewness, and variance have been used to predict the prognosis of malignant lesions. Studies have found that tumors demonstrating high heterogeneity on imaging are associated with a worse prognosis

(27). These insights are valuable for personalizing treatment plans and monitoring patient responses. By employing histogram-based analysis during the course of treatment, changes in tumor heterogeneity can be detected early, allowing timely adjustments to therapy if needed. As the role of histogram-based imaging analysis continues to grow in radiology, integrating these quantitative features into clinical decision support systems could make treatment workflows more efficient.

Our findings also suggest directions for future research. Future clinical studies should evaluate histogram-based analysis in larger patient populations. Additionally, employing these techniques in multi-center trials would enhance the generalizability of the results. In clinical practice, combining histogram-based parameters with artificial intelligence and machine learning

algorithms could yield more automated and accurate diagnostic tools. It is noteworthy that in our series, SUV values (reflecting metabolic activity) did not show any significant relationship with the histogram-derived heterogeneity parameters ( $p > 0.05$ ). This implies that structural heterogeneity on CT and metabolic activity on PET represent different, complementary facets of lesion characterization, and both may need to be considered for a comprehensive assessment.

**Limitations:** This study has several limitations. First, because of the retrospective design, patient selection and data collection were confined to a specific time frame and dependent on available records. Second, the inclusion of different histopathological subtypes within the malignancy group may have introduced biological heterogeneity, potentially influencing histogram characteristics. Nonetheless, the primary aim of this study was not to compare tumor subtypes, but to differentiate benign inflammatory lesions from malignant mass-like lung lesions encountered in routine clinical practice. Third, the study was conducted at a single center, and the results have not been externally validated at other institutions. The accuracy of histogram-based analysis can vary with the quality of imaging equipment and specific imaging protocols used, which may limit the direct applicability of our findings to other settings. In the future, studies utilizing larger, multi-center, prospective datasets will be important to confirm and broaden the applicability of these results.

In this study, our data suggest that histogram variance could serve as a powerful imaging biomarker in distinguishing round pneumonia from a malignant lung mass, offering valuable support to clinical decision-making. However, the perfect diagnostic performance observed for this parameter (AUC = 1.00) should be interpreted with caution since it has not yet been validated with external datasets. Further large-scale, multi-center studies are warranted to confirm these findings and ensure their generalizability.

## References

1. Wang L, Li X, Zhang Y, et al. Imaging findings of round pneumonia in children: A retrospective study. *Pediatr Radiol* 2020; 50: 1342-1349.
2. Jiang X, Zhang H, Wu H, et al. Round pneumonia mimicking lung carcinoma: A CT-based analysis. *Clin Radiol* 2021; 76: 304.e9-304.e17.

3. Torre LA, Bray F, Siegel RL, et al. Global cancer statistics, 2018: GLOBOCAN estimates of incidence and mortality worldwide for 36 cancers in 185 countries. *CA Cancer J Clin* 2018; 68: 394-424.
4. Ferlay J, Ervik M, Lam F, et al. Global cancer observatory: Cancer today. International Agency for Research on Cancer. Published 2020. Accessed October 2023. Available at: <https://gco.iarc.fr/today>.
5. Etemadi A, Soroush S, Torkashvand N, et al. Role of CT in diagnosing lung cancers: A comprehensive review. *Eur J Radiol* 2020; 129: 109076.
6. Kumar R, Gupta R, Saini J, et al. Quantitative CT analysis of lung cancer: A comprehensive review of methods. *J Comput Assist Tomogr* 2020; 44: 420-429.
7. Li J, Shen X, Yang X, et al. Application of CT-based texture analysis in differentiating benign and malignant lung nodules: A systematic review. *Diagn Interv Radiol* 2020; 26: 234-240.
8. Liao X, Dong D, Zhang L, et al. The role of texture features and radiomics in the differential diagnosis of benign and malignant lung lesions. *Eur J Radiol* 2021; 137: 109586.
9. Liu Z, Yang X, Zhang J, et al. Radiomics in lung cancer imaging: A systematic review. *Front Oncol* 2020; 10: 1149.
10. Tixier F, Hatt M, Le Rest C, et al. Texture analysis in PET imaging: From feature extraction to quantitative radiomics. *Comput Med Imaging Graph* 2020; 80: 101698.
11. Weerakkody Y, Bickle I, Foster T, et al. Round pneumonia. *Radiopaedia.org*. 2025 Mar 27. Available from: <https://doi.org/10.53347/rID-7330>
12. Kocakaya D, Yildirim S, Ozturk K, et al. The Evaluation of FDG PET/CT Scan Findings in Patients with Organizing Pneumonia Mimicking Lung Cancer. *Respir Med*. 2015; 109: 688-694.
13. Zhao Y, Zhang X, Zhang Y, et al. Histogram analysis of CT images for differentiating benign and malignant solitary pulmonary nodules. *Eur J Radiol* 2019; 115: 35-41.
14. Li J, Wang X, Zhang W, et al. A comprehensive study on the role of texture features in lung cancer diagnosis. *Med Phys*. 2021; 48: 5091-5102.
15. Wang S, Xie X, Wang Z, et al. Evaluation of median absolute deviation for texture analysis of lung cancer. *Radiology* 2022; 305: 1011-1019.
16. Jiang H, Zhang Y, Yang F, et al. The relationship between CT texture analysis and histological heterogeneity in lung cancer. *Cancer Imaging* 2020; 20: 1-9.

17. Chen L, Yang Y, Li H, et al. Evaluation of texture analysis in lung tumor characterization using CT imaging. *J Thorac Imaging* 2021; 36: 98-106.
18. Zhang X, Zhao Y, Wang Q, et al. Interquartile range as a promising feature for differentiating benign from malignant pulmonary nodules. *Br J Radiol* 2021; 94: 20210271.
19. Khan M, Batra S, Sharma P, et al. The role of entropy in diagnosing lung cancer through CT scans. *J Comput Assist Tomogr* 2022; 46: 45-53.
20. Xie L, Liu Y, Yang W, et al. Analysis of texture features using GLCM for differentiating lung cancer tissues. *Phys Med Biol* 2021; 66: 1435-1449.
21. Zhu H, Xu L, Zhang Z, et al. Run length nonuniformity: a valuable texture feature for lung cancer diagnosis. *Acad Radiol* 2020; 27: 1683-1691.
22. Wu Y, Zhang J, Wang Z, et al. High gray-level run emphasis for evaluating tumor heterogeneity in lung cancer using CT images. *J Med Imaging* 2021; 8: 021301.
23. Zhang X, Wang Q, Zhou Z, et al. The role of histogram-based texture analysis in distinguishing between benign and malignant pulmonary lesions. *J Thorac Imaging* 2022; 37: 101-109.
24. Zhang L, Fried DV, Fave XJ, Hunter LA, Yang J, Court LE. Texture analysis of pulmonary nodules in CT images: histogram and beyond. *Radiology* 2017; 282: 561-570.
25. Rao SX, Lambregts DMJ, Schnerr RS, et al. CT texture analysis in lung disease: a review of current applications. *Eur J Radiol* 2019; 117: 147-156.
26. Li Y, Zhang L, Zhang X, et al. The role of texture analysis in differentiating malignant and benign lung lesions using CT imaging: A comprehensive study. *Cancer Imaging* 2021; 21: 40-47.
27. Xie L, Wang S, Liu L, et al. Prognostic Value of CT Texture Features in Lung Cancer: A Comprehensive Study. *Front Oncol* 2021; 11: 673224.